AIP Advances

RESEARCH ARTICLE | JANUARY 10 2020

A 3D numerical analysis on magnetic field enhanced microwave linear plasma

Special Collection: 2020 Fluids and Plasmas

Wenjin Zhang; Longwei Chen ✉; Yiman Jiang; Chengzhou Liu; Ying Zhao; Jiafang Shan; Fukun Liu

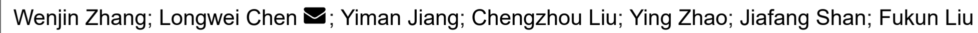

Check for updates

AIP Advances 10, 015220 (2020)
https://doi.org/10.1063/1.5127555

View Online
Export Citation

Articles You May Be Interested In

Characteristics of cylindrical plasma discharge with a thermal electron beam
Phys. Plasmas (September 2016)

A new large area lanthanum hexaboride plasma source
Rev. Sci. Instrum. (August 2010)

On the generation of magnetic field enhanced microwave plasma line
Phys. Plasmas (December 2016)

23 January 2025 08:35:32

AIP Publishing

Special Topics Open for Submissions

Learn More

AIP Publishing

A 3D numerical analysis on magnetic field enhanced microwave linear plasma

Cite as: AIP Advances 10, 015220 (2020); doi: 10.1063/1.5127555
Submitted: 14 September 2019 • Accepted: 17 December 2019 •
Published Online: 10 January 2020

View Online

Export Citation

CrossMark

Wenjin Zhang,[1,2] Longwei Chen,[1,a)] Yiman Jiang,[1] Chengzhou Liu,[1] Ying Zhao,[1,2] Jiafang Shan,[1] and Fukun Liu[1]

AFFILIATIONS

[1] Institute of Plasma Physics, Chinese Academy of Sciences, Hefei 230031, China
[2] University of Science and Technology of China, Hefei 230026, China

[a)] Author to whom correspondence should be addressed: lwchen@ipp.ac.cn

ABSTRACT

Microwave linear plasma has attracted a lot of attention due to the outstanding characteristics such as high electron density, low electron temperature, no-pollution, and homogenization, which can realize a large-area uniform plasma source through vertical or horizontal arrangement especially. In order to explore the effect of the permanent magnets and the microwave coaxial reflective antenna on density and uniformity of plasma, a three-dimensional numerical model is established. It is expected to obtain a superior microwave linear plasma source with high density and uniformity for fabricating a carbon film such as graphene or surface treatment. The results show that (1) permanent magnets can improve the density and uniformity of plasma by generating a suitable magnetic field. At the microwave power of 800 W at 20 Pa, the permanent magnets with 150 kA/m enhance the average electron density by 36.67% and control the relative deviation of electron density within −3% to 1% at an axial distance of 100 mm–300 mm. (2) The reflective antenna can effectively regulate the shape and the uniformity of plasma. The semicylinder reflective antenna realizes the relative deviation of electron density within −2% to 0.5%. Meanwhile, the average electron density increases by 3.75% between an axial distance of 100 mm and 300 mm under a microwave power of 800 W at 20 Pa. (3) The external magnetic field and reflective antenna also have the regulation on heavy particles (Ars) in plasma, which is an important factor for application.

© 2020 Author(s). All article content, except where otherwise noted, is licensed under a Creative Commons Attribution (CC BY) license (http://creativecommons.org/licenses/by/4.0/). https://doi.org/10.1063/1.5127555

23 January 2025 08:35:32

I. INTRODUCTION

Microwave discharge plasma is widely applied in the field of material synthesis, surface modification, etc.,[1–6] because of many outstanding characteristics such as high electron density, stability, no-pollution, and good controllability.[7,8] In 1997, Petasch *et al.*[9] designed a device to generate microwave plasma that expanded linearly which tends to achieve outstanding axial uniformity of electron density. The two microwaves are launched from both sides of the waveguide consisting of a copper rod and a quartz tube in a vacuum chamber. The microwave mainly propagates along the waveguide, producing axial homogeneous plasma along the surface of the quartz.[10] In recent years, this linear microwave plasma attracted a lot of attention because of its predominant uniformity for large area plasma treatment such as coating, etching, and cleaning.[11–14] In addition, this linear microwave plasma source is conducive to realize two-dimensional plasma by arranging individual sources in parallel.[15] At present, the experimental applications of microwave linear plasma have made great progress. Kormka *et al.*[12] grew thin diamond films over large areas (up to 20 × 10 cm^2) via linear microwave plasma CVD at 2 mbar. Yamada *et al.*[15] obtained high quality and large area graphene films by combining several linear microwave plasma sources in the roll-to-roll process under the pressure of 30–300 pa.

It is known that an external magnetic field effectively promotes plasma density.[16–18] This is mainly because the magnetic field can increase the efficient collision frequency of the charged particles in a specific region under the effect of the Lorenz force. In applications of microwaves, the magnetic field also plays a significant role. Schlemm *et al.*[19] found that the magnetic field can enhance linear microwave PECVD of Si_3N_4 on multicrystalline solar cells and achieve industrial deposition dimensions over long time. Kato[20] investigated stabilization of the plasma and obtained a high density under a low gas pressure by applying a longitudinal magnetic field. Ganesan *et al.*[21]

© Author(s) 2020

proved that the external magnetic field could increase the density of the plasma and aluminum deposition rate in HIPIMS.

During the producing process of microwave plasma, a microwave antenna has an obvious regulation on plasma by different types. Through introduction of different kinds of antennas,[22–24] the microwave plasma we need can be acquired. Xiaobao *et al.*[25] developed a large area microwave plasma by using the slot antenna and the maximum ion density was 4.3×10^{16} m^{-3} at 400 Pa. Kanoh *et al.*[26] obtained a stable and uniform argon plasma with electron density in the order of 10^{17} m^{-3} by introducing the optimized slot antenna at a processing pressure of 70 Pa. Obrusník and Bonaventura[23] demonstrated the influence of the antenna shielding on the hydrogen plasma and particles by a mixed 2D/3D fluid model.

In order to better explore effects of different conditions on plasma parameters and exploit a plasma source with high density and uniformity simultaneous for application, we build the 3D model using *COMSOL Multiphysics* software. The general structure of this paper is as follows. In Sec. II, the 3D numerical model and simulation conditions are presented. In Sec. III, the results of numerical analysis are showed, including the influence of the permanent magnets and the antenna reflector. Finally, a brief summary is given in Sec. IV.

II. 3D MODEL BUILDING

A. Concept of 3D model

The axial and radial schematic diagrams of the device and 3D numerical model in this paper are shown in Figs. 1(a)–1(c), respectively. The main geometric sizes are given.

The reaction chamber is vacuum where the plasma is generated, installing a coaxial waveguide which is composed of an inner copper rod and an outer quartz tube in the chamber. Outside the chamber, the outer quartz tube of the waveguide is replaced with the copper tube. The coaxial reflective antenna located between the copper rod and the outer tube is introduced. Due to the cutoff effect of electromagnetic wave in plasma,[27] high-density plasma present the metallic property reflecting microwave[28] when the electron density is higher than the critical density (7.46×10^{16} m^{-3} for 2.45 GHz). This is the basic and essential principle of the microwave linear plasma.

Double 2.45 GHz microwave powers are launched from two ends of the coaxial waveguide. The region between the inner copper rod and the outer tube is atmospheric air where mainly microwave propagates in. The neutral working gas in the chamber is excited to be plasma by absorbing the microwave energy. The coaxial waveguide here is like the microwave coaxial transmission line where

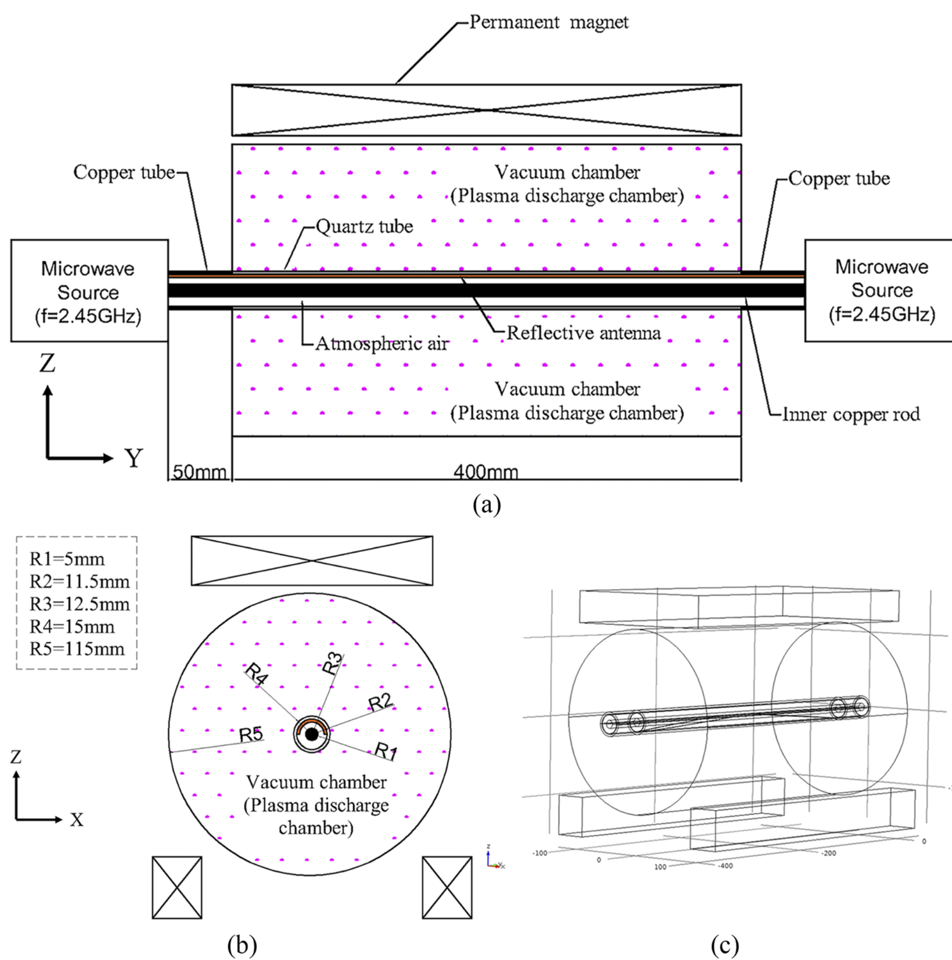

FIG. 1. Schematic diagram of the device: (a) axial, (b) radial, and (c) 3D model.

23 January 2025 08:35:32

© Author(s) 2020

the inner copper rod is like the inner conductor and the high-density plasma generating along the surface of quartz tube is like the outer conductor.[9,10] This mechanism allows microwave to propagate steadily and plasma to extend linearly. The main role of the quartz tube here is isolating the inner copper from the vacuum chamber. Meanwhile, the quartz is the window whose relative permittivity is set to 3.8 in this model for radiating electromagnetic waves. Besides, three permanent magnets are surrounded outside the vacuum chamber to create a suitable magnetic field.

B. Coaxial waveguide

In this model, the coaxial waveguide as shown in Fig. 2(a) is the key to this system. As sated above, the coaxial waveguide in the vacuum chamber consists of the inner copper rod, reflective antenna, and quartz tube. The structure of the reflective antenna can be designed to achieve different requirements; here, we chose the semicylinder as shown in Fig. 2(b). Its material is copper which can reflect microwave energy efficiently. The effect of the reflective antenna on the plasma source will be discussed in detail later.

C. External permanent magnets

In many experiments, the use of the permanent magnets is convenient and drastically reduced the weight of the device. Additionally, the magnetic field strength is adjusted expediently by arranging different numbers of permanent magnets.[29] In this numerical model, the magnetization field of permanent magnets in this model is in the positive z-direction for all three permanent magnets' elements. Figure 3 reveals the distribution of the magnetic field generated by three permanent magnets with 150 kA/m in this 3D model. The value here is the amplitude of magnetic flux. The magnetic field is calculated first serving as the initial value for the microwave plasma element in this simulation.

D. Numerical model definition

1. Physical model

Substantially, the 3D model simulation in this work is the coupling among the three physical fields which are magnetic field, plasma, and microwave field.

The electric field in the microwave model satisfies the following wave equation deduced from Maxwell's equations:

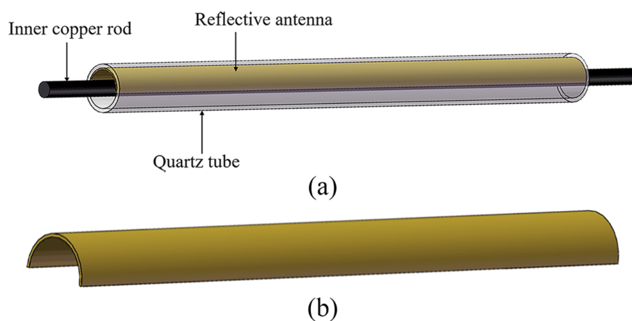

FIG. 2. Schematic diagram of (a) coaxial waveguide and (b) reflective antenna.

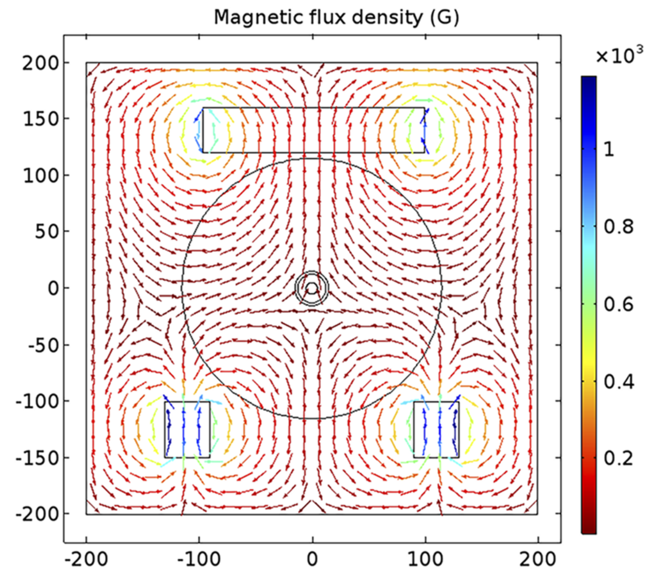

FIG. 3. Distribution of magnetic flux density generated by permanent magnets. Magnetization = 150 kA/m (z-x plane, y = 200 mm).

$$\nabla \times \mu_0{}^{-1}(\nabla \times E) - \omega^2 \varepsilon_{rp} \varepsilon_0 \cdot \mathrm{E} = 0, \tag{1}$$

where μ_0 is $4\pi \times 10^{-7}$ N/A^2 and ε_0 is 8.854×10^{-12} F/m, which are the permeability and the permittivity in vacuum, respectively. ω is the angular frequency, i.e., 2π × 2.45 GHz. ε_{rp} is the relative permittivity which depends on the characteristics of materials. In this model, the relative permittivity of quartz and air is set to 3.8 and 1, respectively. However, for plasma, there is no constant that can be responsible for the relative permittivity. In the absence of the external magnetic field, the relative permittivity of plasma can be approximately expressed as[30]

$$\varepsilon_{rp} = 1 - \frac{\omega_{pe}^2}{\omega(\omega - j\nu)}. \tag{2}$$

Here, j is the imaginary symbol and v is the collision frequency of electron-neutral particles. ω_{pe} denotes the plasma oscillation frequency that depends on the plasma density n_e,

$$\omega_{pe} = \left(\frac{e^2 n_e}{\varepsilon_0 m}\right)^{1/2}, \tag{3}$$

where m and e are the electron mass and electron charge, respectively.

For unmagnetized plasma, the conductivity δ is as follows:

$$\sigma = \frac{\varepsilon_0 \omega_{pe}^2}{j\omega + \nu}. \tag{4}$$

Equation (2) can be written as follows:

$$\varepsilon_{rp} = 1 - \frac{j\sigma}{\varepsilon_0 \omega}. \tag{5}$$

23 January 2025 08:35:32

© Author(s) 2020

For magnetized plasmas, the relative dielectric property should be expressed in full tensor.[30]

In this model, the magnetic field is generated by permanent magnets described by the following equations:

$$\nabla \times H_s = 0, \tag{6}$$

$$H_s = -\nabla V_m. \tag{7}$$

Here, Hs is the intensity of the magnetic field and V_m is the scalar magnetic potential.

Using the constitutive relationship between magnetic flux density and magnetic field, the following equations are solved:

$$B_s = \mu_0 (H_s + M), \tag{8}$$

$$\nabla \cdot B_s = 0, \tag{9}$$

where B_s is the magnetic flux density. M is the magnetization field which is the direct parameter of permanent magnets.

In the presence of the magnetic field, the plasma conductivity σ should be expressed in full tensor. Using the definition $\boldsymbol{\alpha} = \frac{e}{m(v+j\omega)}$, the inverse plasma conductivity can be expressed as follows:

$$\sigma^{-1} = \frac{1}{\alpha q n_e}\begin{vmatrix} 1 & -\alpha B_{sz} & \alpha B_{sy} \\ \alpha B_{sz} & 1 & -\alpha B_{sx} \\ -\alpha B_{sy} & \alpha B_{sz} & 1 \end{vmatrix}, \tag{10}$$

where B_{sx}, B_{sy}, B_{sz} are three components of the external magnetic field in x, y, and z directions, respectively.

In the microwave plasma model, the electron density can be obtained by follow continuality equations:[31]

$$\frac{\partial n_e}{\partial t} + \nabla \cdot \Gamma_e = R_e - (u \cdot \nabla) n_e, \tag{11}$$

$$\Gamma_e = -(\mu_e \cdot E_s) n_e - D_e \cdot \nabla n_e. \tag{12}$$

Here, R_e is the electron rate expression. u denotes the neutral fluid velocity vector. It is known that the gas flow may have an effect on the spreading of neutrals and uniformity. The gas temperature is normally high and changed in the microwave discharge experiment which is usually controlled steadily by the pulse power. However, in this work, in order to simply the model of coupling among the three physics fields, the neutral fluid velocity vector and gas temperature are set to zero and 300 K, respectively. E_s represents the electrostatic space-charge field; μ_e is the electron mobility which is a full tensor under the magnetic field as follows:

$$\mu_e{}^{-1} = \begin{vmatrix} \frac{1}{\mu_{dc}} & -B_{sz} & B_{sy} \\ B_{sz} & \frac{1}{\mu_{dc}} & -B_{sx} \\ -B_y & B_{sx} & \frac{1}{\mu_{dc}} \end{vmatrix}, \tag{13}$$

where μ_{dc} is the electron mobility in the absence of a magnetic field which is computed from[27]

$$\mu_{dc} = \frac{e}{mv}, \tag{14}$$

where v is computed from[27]

$$\boldsymbol{v} = 1.52 \times 10^7 p\sqrt{T_e}. \tag{15}$$

Here, p is the working gas pressure and T_e is the electron temperature in electon volts.

The electron energy density is given by the following equations:

$$\frac{\partial n_\varepsilon}{\partial t} + \nabla \cdot \Gamma_\varepsilon + E_s \cdot \Gamma_e = S_{en} - (u \cdot \nabla) n_\varepsilon + Q/e, \tag{16}$$

$$\Gamma_\varepsilon = -(\mu_\varepsilon \cdot E_s) n_\varepsilon - D_\varepsilon \cdot \nabla n_\varepsilon. \tag{17}$$

Here, n_ε and S_{en} are the electron energy density and energy loss/gain from inelastic collisions, respectively; Q is the heat source for plasma due to the electromagnetic waves; and ρ_v is the space charge density. The electron diffusivity De, energy mobility μ_ε, and energy diffusivity D_ε are calculated from the electron mobility using Einstein's relation,[18]

$$D_e = \mu_e T_e, \mu_\varepsilon = \left(\frac{5}{3}\right)\mu_e, D_\varepsilon = \mu_\varepsilon T_e. \tag{18}$$

The following equation is solved for the mass fraction of heavy species:[32]

$$\rho \frac{\partial}{\partial t}\omega_k + \rho(u \cdot \nabla)\omega_k = \nabla \cdot j_k + R_k, \tag{19}$$

where ω_k, j_k, R_k, u, and ρ represent the mass fraction of heavy species, diffusive flux vector, rate expression for species k, fluid velocity vector, and density of the mixture, respectively.

For a more detailed explanation of the equations, the reader can refer to Refs. 30 and 31.

2. Species and reactions

To simplify the model, argon is selected as the working gas, assuming only four species exist in the plasma discharge chamber, i.e., electrons (e−), ground state atoms (Ar), metastable particles (Ars), and ions (Ar+).[33] Under this assumption, the argon plasma chemistry with the following set of collisions and reactions is shown in Tables I and II including elastic, excitation, direct ionization, stepwise ionization,[34] and so on.

3. Boundary conditions

Essentially, the model is made up of many partial differential equations, which must be supplemented with a suitable set of

TABLE I. Collisions and reaction.

Reaction	Formula	Type	Δε (eV)
1	e + Ar ⇒ e + Ar	Elastic	0
2	e + Ar ⇒ e + Ars	Excitation	11.5
3	e + Ars ⇒ e + Ar	Superelastic	−11.5
4	e + Ar ⇒ 2e + Ar^+	Ionization	15.8
5	e + Ars ⇒ 2e + Ar^+	Ionization	4.24
6	Ars + Ars ⇒ e + Ar + Ar^+	Penning ionization	...
7	Ars + Ar ⇒ Ar + Ar	Metastable quenching	...

TABLE II. Surface reactions.

Reaction	Formula	Sticking coefficient
1	Ar+ ⇒ Ar	1
2	Ars ⇒ Ar	1

23 January 2025 08:35:32

© Author(s) 2020

boundary conditions. In this 3D model, the microwave plasma is solved in the domain of the plasma discharge chamber and coaxial waveguide,[32] except for the metal domain. The inner copper rod, the reflective antenna, and the wall of the chamber are perfect electric conductors, and among them, the wall is grounded. The boundary conditions of the two microwave ports are used to drive the electromagnetic waves by different powers which are coaxial incentive. The glass tube in the coaxial waveguide is insulation. The three permanent magnets outside the vacuum chamber will produce a magnetic field extending to infinity. Thus, for calculating the magnetic field, a sufficiently large peripheral air domain whose boundary condition is set to the infinite element layer is used to encase the whole 3D model.

In this model, the reaction chamber (radius: 115 mm) is much larger than the size of the quartz tube (radius: 15 mm). The high density of plasma is generated along the surface of the quartz tube. Therefore, the secondary electrons on the wall have a weak effect on the result which is not discussed in this model.

III. RESULTS AND DISCUSSION

Based on the 3D model presented above, numerical research has been performed to analyze the influence of external permanent magnets and reflective antenna on the plasma. For intuitively and conveniently expressing the physical phenomena obtained, the following data analysis was all selected from the y-z axis cut plane (x = 0) of the 3D model.

The results of similar works of Petasch *et al.*[9] and Hübner *et al.*[35] are compared to verify our 3D numerical model. Herein, the comparison of results under different conditions is shown in Figs. 4(a) and 4(b). In Fig. 4(a), the axial electron density at different distances from the quartz tube wall is measured at the power of 210 W under the gas pressure of 50 Pa, where L is the length of the plasma line. The results of the numerical model show an excellent axial homogeneity which are in agreement with the work of Petasch. In Fig. 4(b), the radial plasma density is obtained at 100 Pa in dependence of different microwave powers. Both in the numerical model and the reference work, radial plasma density decays as radial distance increases and increases with improvement of microwave power. In general, the results from the 3D numerical model reveal consistent trends with two reference works which confirm that this 3D model has a guidance value for experiments and applications.

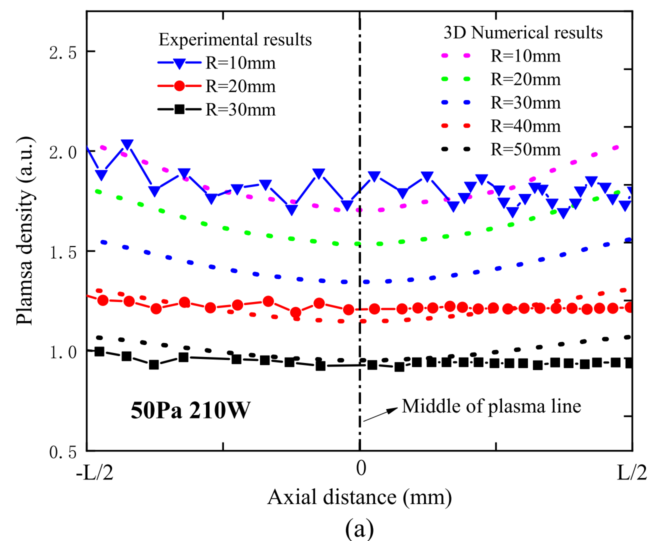

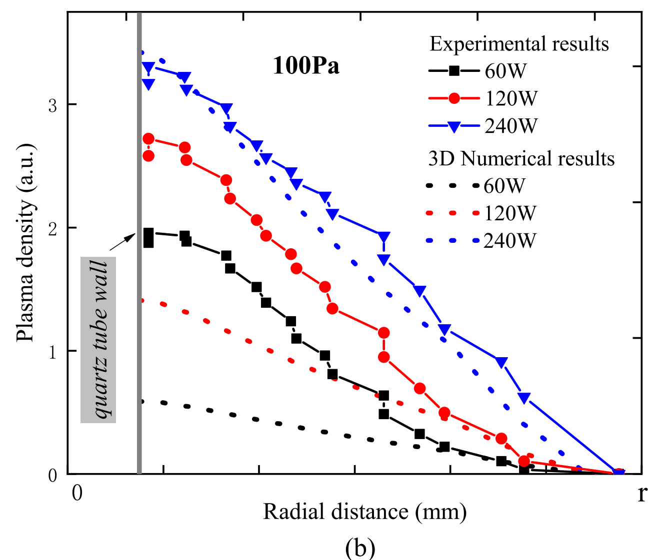

FIG. 4. Comparisons between the 3D numerical model and the works of (a) Petasch *et al.*[9] (R is the distance from the quartz tube wall) and (b) Hübner *et al.*[35]

A. Effect of reflective antenna

Figures 5(a) and 5(b) show the distribution of electron density at 20 Pa without and with reflective antenna, respectively. The microwave reflective antenna has an obvious effect on the shape of plasma. Without the reflective antenna, the high-density electron is concentrated in the two ends of the coaxial waveguide where the electromagnetic waves are launched. After adding the reflective antenna, the high-density plasma is linearly distributed along the axial direction at the downstream area, which is in accordance with the numerical results shown in Figs. 6(a)–6(d).

Here, we measured the plasma density without and with a reflective antenna in the dependence of microwave power. In Fig. 6(a), the axial plasma density without a reflective antenna decreases in the middle of the axis, which is compensated and equally distributed after adding a semicylindrical reflective antenna in Fig. 6(c). As the variation of radial density shown in Fig. 6(d), the high-density plasma is concentrated at the opening of the reflective antenna due to the concentration of the microwave energy. In this case, most of the microwave is reflected to emit into the downstream region in the chamber, where more neutral particles are excited to be plasma. The reflective antenna concentrates the microwave energy at the opening and weakens the evanescent mode of the electromagnetic wave. At the same time, the microwave energy propagates continually forward, which improves the uniformity of plasma. It can be considered that the semicylindrical

23 January 2025 08:35:32

© Author(s) 2020

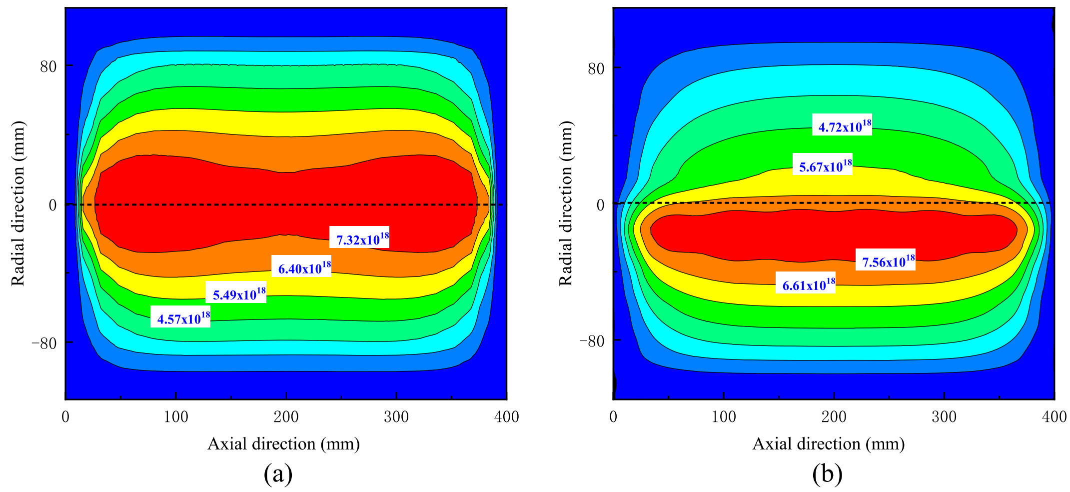

FIG. 5. Distribution of plasma density (a) without and (b) with a reflective antenna under a microwave power of 800 W without a magnetic field (20 Pa, y-z plane at x = 0).

FIG. 6. Trend of axial (r = −50 mm) and radial (z = 100 mm) electron density [(a) and (b)] without and [(c) and (d)] with a reflective antenna under different microwave powers without a magnetic field (20 Pa).

23 January 2025 08:35:32

© Author(s) 2020

reflective antenna plays an effective role in optimization of uniform plasma.

B. Effect of permanent magnets

It is known that the electrons will make a whirling motion along the magnetic field line under the action of the Lorentz force when a magnetic field is presented.[27] The simulation results of the three permanent magnets in Fig. 3 show that there is high density magnetic flux in the position of the vacuum chamber. The electrons and ions in the chamber will do the Larmor gyration in the magnetic field increasing the collision frequency of electrons.[8]

From the results in Figs. 7(a)–7(d), it is found that the magnetic field can both improve the density and uniformity of plasma.[36] Through further exploration on the internal physical mechanism, it is indicated that the peripheral magnetic field reduces the attenuation of the microwave in the axial direction, which has a considerable effect on the energy transmission of microwave linear plasma.[18]

Both axial and radial electron density rise distinctly with the increase in the magnetization field of permanent magnets. In Fig. 7(a), the plasma density in the middle of the axial direction increases under the effect of the magnetic field, which is mostly due to the small attenuation of the electromagnetic wave.[18] This means that the microwave energy fed from both ends of the waveguide can propagate further along the axial direction. Under this mechanism, the microwave energy is compensated in the middle of the axis, and the electron density is improved. When the reflective antenna is introduced, the uniformity of electron density is distinct with the enhancement and confinement from the magnetic field.

Microwave linear plasma is a very popular and excellent method in the area of materials preparation, surface treatment, and

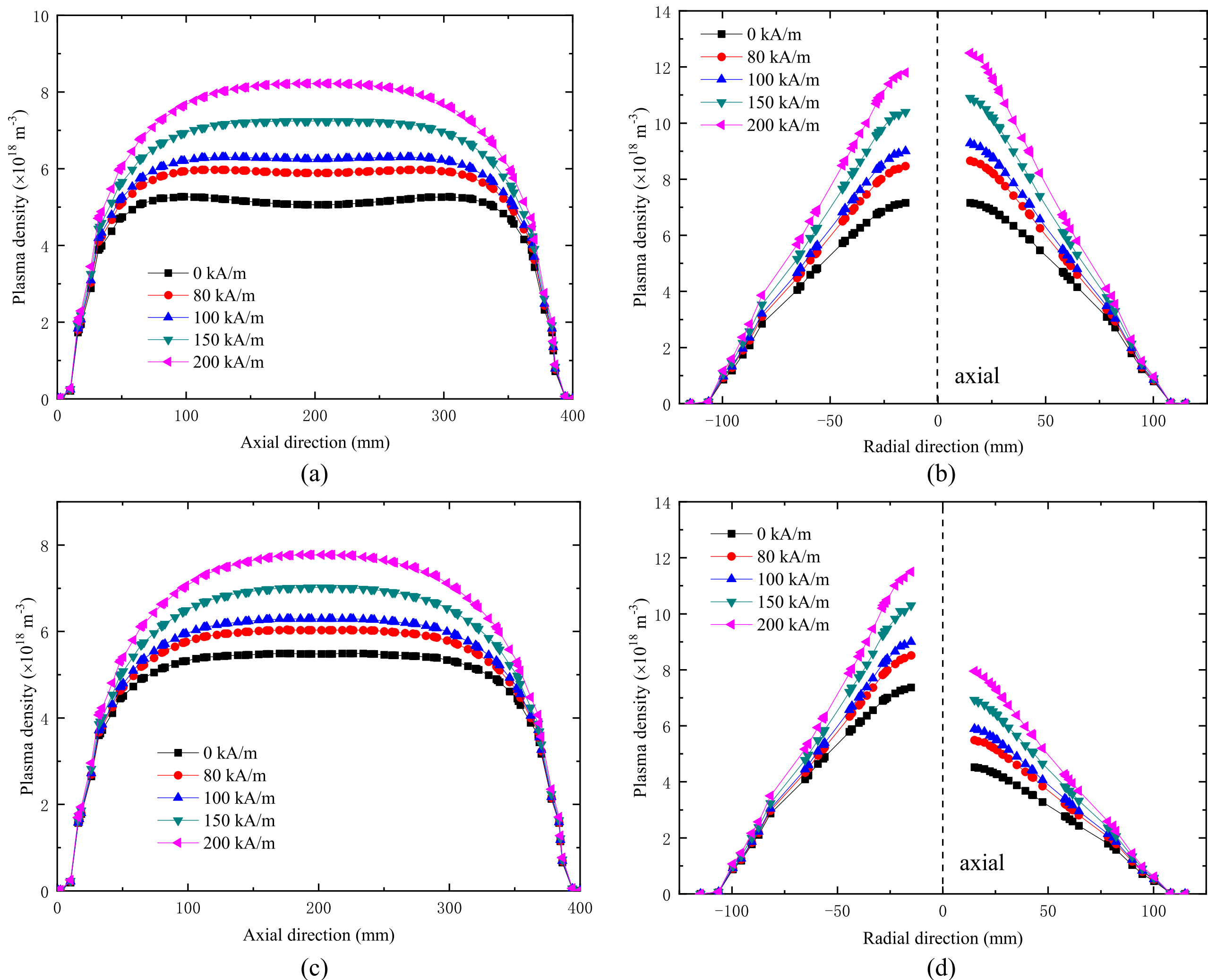

FIG. 7. Axial (r = −50 mm) and radial (z = 100 mm) plasma density [(a) and (b)] without and [(c) and (d)] with the reflective antenna under different magnetizations of magnets at a power of 800 W. (20 Pa.)

23 January 2025 08:35:32

© Author(s) 2020

other applications.[12,19,37] Then, how to obtain a microwave linear plasma source with high-density and good uniformity simultaneously has always been the goal pursued by researchers. Herein, the concepts of the relative deviation and amplification in statistics are utilized to analyze the uniformity of the magnetic field enhanced microwave linear plasma source in this model. The average value X is the arithmetic average of original data on the specified line selection which comes from numerical simulation directly. The relative deviation and amplification can be described by the following equations:

$$\varphi = \frac{d}{X} \times 100\%. \tag{20}$$

Here, φ is the relative deviation and d is the difference between the value of each electron density and the average electron density,

$$A = \frac{X - X_0}{X_0} \times 100\%. \tag{21}$$

Here, A is the amplification of average density. X_0 is the cardinal number. Here, the cardinal number is the average density at 800 W without a magnetic field and antenna reflector, which is $5.26 \times 10^{18}\ \mathrm{m}^{-3}$.

In Fig. 8(a), relative deviations of electron density in different axial distances under 800 W are presented. At a power of 800 W, with the axial distance between two ends becoming shorter, the electron density deviation is closer to 0%. After that, the axial distance of 100 mm–300 mm with a desirable uniformity and an acceptable effective length which accounts for 50% of the length of the coaxial waveguide is selected to analyze the effect of different conditions. From the results presented in Fig. 8(b), the relative deviation of plasma density under different magnetization intensity in the axial distance of 100 mm–300 mm is explored. It is apparent that the attenuation of the electromagnetic wave is alleviated as the magnetization increases. Meanwhile, the uniformity between the axial distance of 100 mm and 300 mm increases and then declines. Figure 8(c) shows the amplification of average electron density with promotion of magnetization intensity in the axial distance of 100 mm–300 mm at 800 W. The average plasma density almost linearly increases with the magnetic field intensity. The amplification here is relative to the average electron density at 800 W without a magnetic field and antenna reflector, calculated by Eq. (21). When the magnetization of magnets is 150 kA/m, the average plasma density reaches $7.18 \times 10^{18}\ \mathrm{m}^{-3}$, and the electron density in the middle of the axis starts higher than the average value.

After the above analysis, a discussion on the relative deviation of electron density under different conditions between the axial distance of 100 mm and 300 mm at 800 W is performed, and the results are shown in Figs. 9(a)–9(d). Figures 9(a)–9(d) show the distribution of the electron density and the trend of relative deviation under different conditions, where the red dotted line corresponds to the value of average electron density of an axial distance of 100 mm–300 mm at the corresponding condition. In Fig. 9(a), the electron density between the axial distance of 150 mm and 250 mm is lower than the average value due to the fading of the microwave. The relative deviation is from −2% to 2%, which indicates that dual microwave sources are insufficient to offset the energy attenuation during transmission of waves. However, in Fig. 9(b), after adding an external magnetic field, the average electron density is significantly improved,

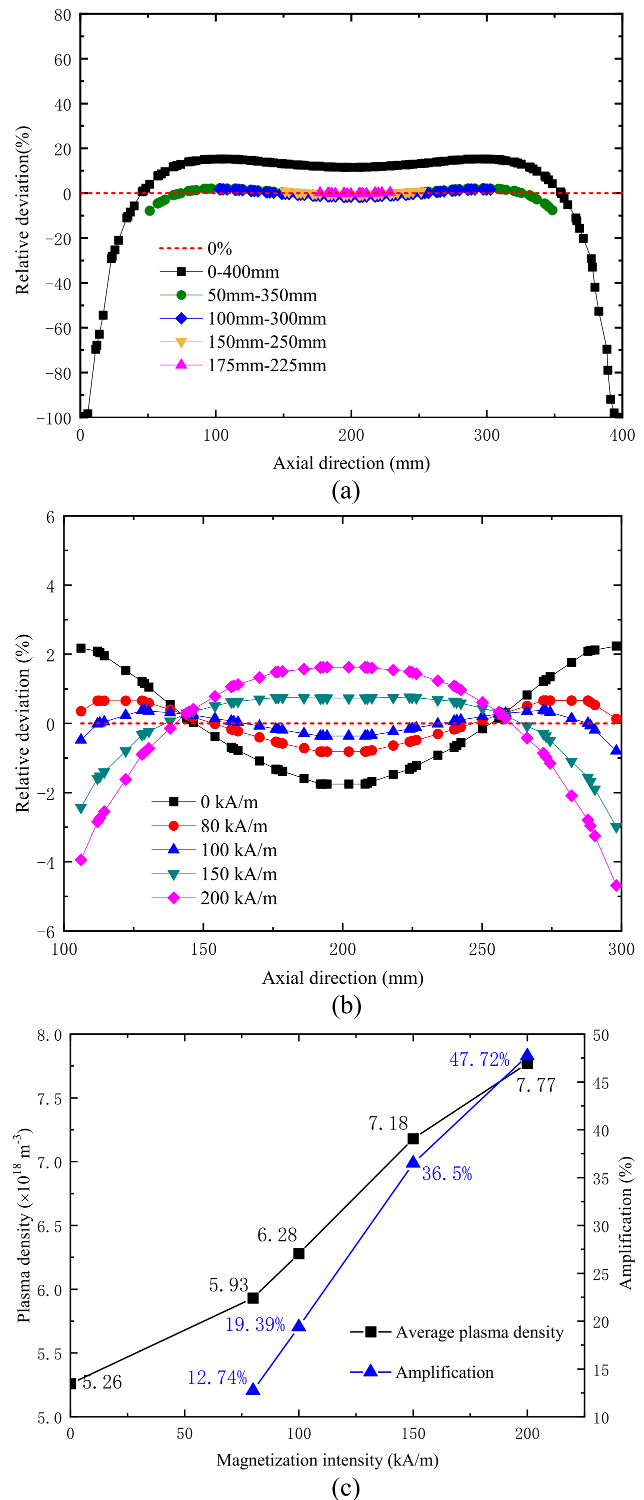

FIG. 8. (a) Relative deviations of electron density in different axial distances under 800 W. (b) Relative deviation of electron density and (c) amplification of average electron density in the axial distance of 100 mm–300 mm at 800 W under different magnetizations (r = −50 mm).

23 January 2025 08:35:32

© Author(s) 2020

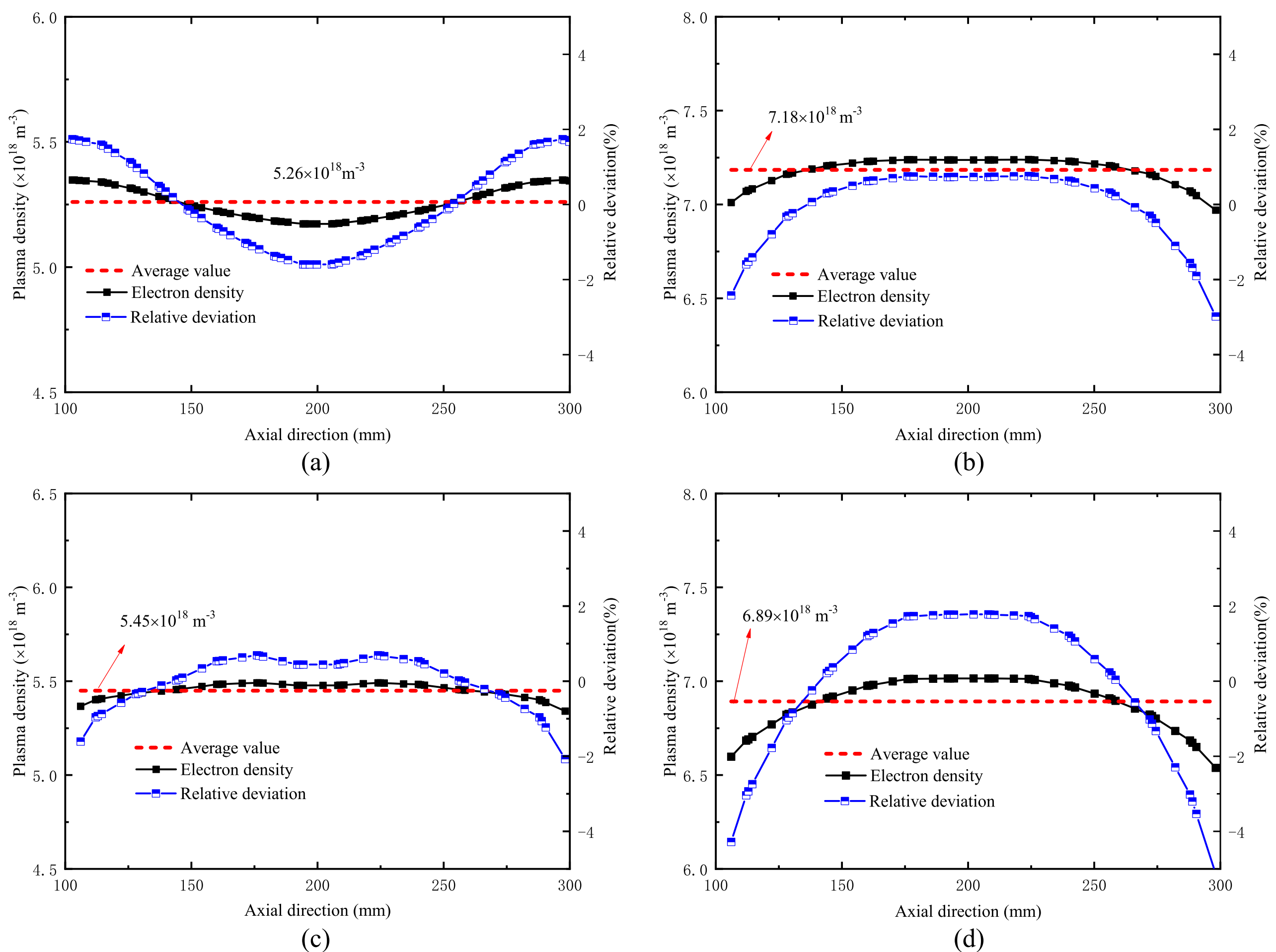

FIG. 9. Relative deviation and distribution of electron density in the axial distance of 100 mm–300 mm (r = −50 mm): (a) power of 800 W; (b) power of 800 W and magnetization of 150 kA/m; (c) power of 800 W and reflective antenna; and (d) power of 800 W and magnetization of 150 kA/m and reflective antenna.

23 January 2025 08:35:32

especially in the axial middle portion where the density is higher than the average. At the same time, the relative deviation becomes smaller, which demonstrates that the action of the magnetic field is not only on electron density but also on the uniformity of plasma as mentioned above.

Figure 9(c) is the variation of electron density after introducing the semicylindrical antenna reflector. The original data is distributed smoothly, and the relative deviation is narrowed in −2% to 0.5%. On this basis, the magnetic field generated by the three magnets with 150 kA/m is added to obtain the result shown in Fig. 9(d). The average electron density is increased by the combination of the magnetic field and the antenna reflector. However, the relative deviation of the density is amplified from −4% to 2%, spanning six percentages.

By the analysis above, we make a brief summary shown in Table III. The data in Table III show that both permanent magnets and reflective antenna in this 3D model can increase the plasma density. Among them, the external magnetic field has a prominent enhancement on plasma density. Under the magnetic field generated by permanent magnets with 150 kA/m, the amplification of average density achieves 36.67% at 800 W. Additionally, the relative deviation of electron density is narrowed in −2% to 0.5% with the effect of the semi-cylindrical reflective antenna under the microwave power of 800 W, which has an outstanding optimization on plasma uniformity. However, it should be noticed that when the magnetic field and the reflective antenna are added at the same time, the average plasma density is higher than introducing the antenna reflector separately but lower than the individual addition of the permanent magnets. Besides, we obtained the results of average power absorbed per electron. It is found that the average power absorbed per electron increases after adding the reflective antenna but decreases in the presence of the external magnetic field. This is due to the energy transduction between electron and neutral particles under the high collision frequency increased by the external magnetic field. The concentration of the microwave by the reflective antenna promotes the absorption of energy by electrons.

Actually, in the microwave discharge plasma, the distribution of heavy particles (Ars) is very important for application of materials and surface treatment.[38] Therefore, the results on heavy

© Author(s) 2020

TABLE III. Conditions and results (axial distance of 100 mm–300 mm).

Conditions	Average electron density ($\times 10^{18}$ m^{-3})	Amplification (%)	Relative deviation (%)	Average power absorbed per electron (W)
800 W	5.26	...	−2 to 2	1.98
800 W + 150 kA/m	7.18	36.67	−3 to 1	1.91
800 W + reflective antenna	5.45	3.75	−2 to 0.5	2.05
800 W + 150 kA/m + reflective antenna	6.89	31.12	−5 to 2	1.93

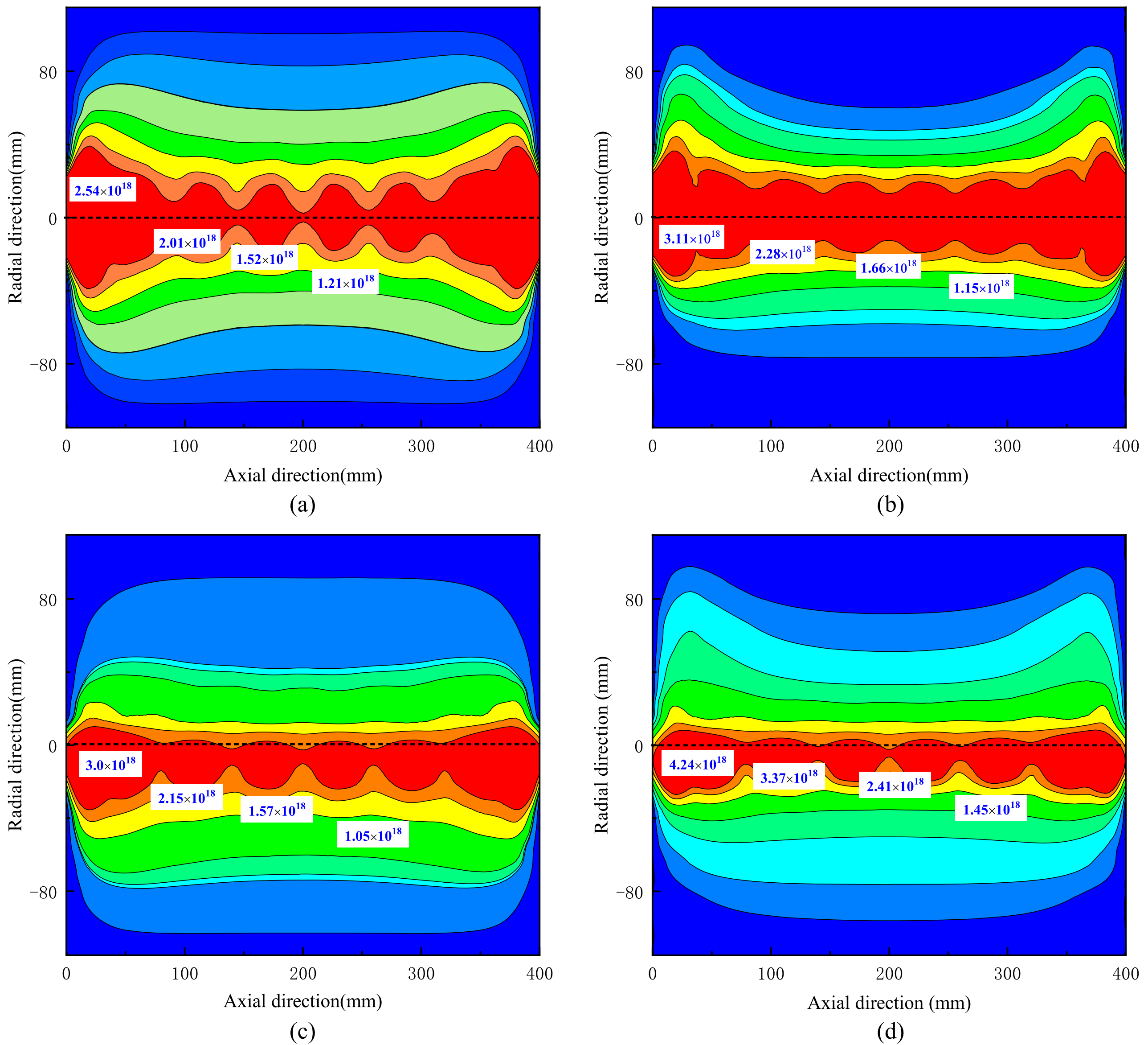

FIG. 10. Distribution of heavy particles (Ars) (20 Pa, y-z plane, x = 0): (a) power of 800 W; (b) magnetization of 150 kA/m; (c) reflective antenna; and (d) magnetization of 150 kA/m and semicylindrical antenna reflector.

23 January 2025 08:35:32

© Author(s) 2020

particles (Ars) under following four conditions are analyzed, as shown in Figs. 10(a)–10(d). On the account of the large mass, the drift diffusion velocity of heavy particles (Ars) is much slower than that of electrons.[39] The different diffusion velocity causes different responses to the fast change in the electric field since the microwave frequency of 2.45 GHz is adopted in this model. In that case, the standing wave effect is presented clearly in the distribution of heavy particles. It can be seen intuitively from the cloud diagram that the magnetic field and the reflective antenna both have a direct influence on heavy particles (Ars), which means that the regulation can be achieved.

IV. CONCLUSIONS

In summary, a numerical analysis of a 3D model on magnetic field enhanced linear microwave plasma is performed. The influences of external permanent magnets and a reflective antenna on plasma are discussed. The external magnetic field generated by permanent magnets has an advantageous effect on the density and uniformity of plasma, the same as with the microwave reflective antenna. Under the microwave power of 800 W and gas pressure of 20 Pa, the magnetic field generated by permanent magnets with 150 kA/m can raise the average plasma density between the axial distance of 100 mm and 300 mm by 36.67% with the relative deviation of density of −3% to 1%. On the same conditions of gas pressure and microwave power, the semicylindrical reflective antenna can control the uniformity of plasma density between the axial distance of 100 mm and 300 mm within −2% to 0.5% with the average density increasing by 3.75%. In addition, the external magnetic field and reflective antenna can also regulate the heavy particles (Ars) in plasma which is an important factor for application. Nevertheless, when the reflective antenna interacts with the magnetic field, the density and uniformity of plasma expressed complicated phenomena. The balance between the function of the antenna reflector and the magnetic field needs further investigation.

In future work, the experiments of the magnetic field enhanced microwave linear plasma will be carried out under the guidance of simulation of this 3D model. The experimental diagnosis by the Langmuir probe and emission spectrum will be proceeded to verify the model and expected to obtain a more excellent plasma source with high electron density and uniformity.

ACKNOWLEDGMENTS

This research was funded by the National Natural Science Foundation (Grant Nos. 11575252 and 11775270) and the Natural Science Foundation of Anhui Province under Grant No. 1708085MA26.

REFERENCES

[1] M. Liehr and M. Dieguez-Campo, Surf. Coat. Technol. **200**(1–4), 21–25 (2005).
[2] H. Li, Ph.D. thesis, University of Science and Technology of China, 2017.
[3] E. Tatarova, J. Henriques, C. C. Luhrs, A. Dias, J. Phillips, M. V. Abrashev, and C. M. Ferreira, Appl. Phys. Lett. **103**(13), 134101 (2013).
[4] E. Tatarova, A. Dias, J. Henriques, A. M. Botelho do Rego, A. M. Ferraria, M. V. Abrashev, C. C. Luhrs, J. Phillips, F. M. Dias, and C. M. Ferreira, J. Phys. D: Appl. Phys. **47**(38), 385501 (2014).
[5] S. Hübner, *Poly-diagnostic study of low pressure microwave plasmas* (Technische Universiteit Eindhoven, 2013).
[6] R. Rincón, C. Melero, M. Jiménez, and M. D. Calzada, Plasma Sources Sci. Technol. **24**(3), 032005 (2015).
[7] H. Conrads and M. Schmidt, Plasma Sources Sci. Technol. **9**(4), 441 (2000).
[8] A. Von Keudell and V. Schulz-Von Der Gathen, Plasma Sources Sci. Technol. **26**(11), 113001 (2017).
[9] W. Petasch, E. Räuchle, H. Muegge, and K. Muegge, Surf. Coat. Technol. **93**(1), 112–118 (1997).
[10] E. Räuchle, J. Phys. IV **08**(PR7), Pr7-99–Pr97-108 (1998).
[11] L. Hui, W. Aimin, Z. Wenlan, L. Wenq, Q. Fuwen, and D. Chuang, J. Harbin Eng. Univ. **36**(3), 423–426 (2015).
[12] A. Kromka, O. Babchenko, T. Izak, K. Hruska, and B. Rezek, Vacuum **86**(6), 776–779 (2012).
[13] W. Yu, Z. Xiao, C. Longwei, M. Yuedong, F. Shidong, S. Jie, and S. Xingsheng, Plasma Sci. Technol. **16**(4), 356–362 (2014).
[14] X. Zuo, C. Longwei, W. Yu, Z. Yin, and M. Yuedong, Appl. Phys. **2**(4), 109–115 (2012).
[15] T. Yamada, M. Ishihara, and M. Hasegawa, Thin Solid Films **532**(532), 89–93 (2013).
[16] T. Lagarde, J. Pelletier, and Y. Arnal, Plasma Sources Sci. Technol. **6**(1), 53 (1997).
[17] J. Yang, Y. Xu, Z. Meng, and T. Yang, Phys. Plasmas **15**(2), 023503 (2008).
[18] L. Chen, Y. Zhao, K. Wu, Q. Wang, Y. Meng, and Z. Ren, Phys. Plasmas **23**(12), 123509 (2016).
[19] H. Schlemm, A. Mai, S. Roth, D. Roth, K. M. Baumgärtner, and H. Muegge, Surf. Coat. Technol. **174-175**, 208–211 (2003).
[20] I. Kato, T. Yamagishi, Y. Morita, and T. Kamiko, Electron. Commun. Jpn. **81**(3), 10–16 (1998).
[21] R. Ganesan, B. Akhavan, X. Dong, D. R. Mckenzie, and M. M. M. Bilek, Surf. Coat. Technol. **352**, 671–679 (2018).
[22] C. F. Wu, R. J. Zhan, X. H. Wen, and W. D. Huang, IEEE Trans. Plasma Sci. **29**(1), 13–18 (2001).
[23] A. Obrusník and Z. Bonaventura, J. Phys. D: Appl. Phys. **48**(6), 065201 (2015).
[24] F. Fendrych, A. Taylor, L. Peksa, I. Kratochvilova, J. Vlcek, V. Rezacova, V. Petrak, Z. Kluiber, L. Fekete, and M. Liehr, J. Phys. D: Appl. Phys. **43**(37), 374018 (2010).
[25] S. Xiaobao, W. Qinchong, W. Yuanxi, L. Rongqing, and S. Yifeng, Nucl Fusion Plasma Phys. **19**(1), 16–20 (1999).
[26] M. Kanoh, K. Aoki, T. Yamauchi, and Y. Kataoka, Jpn. J. Appl. Phys., Part 1 **39**(9), 5292–5296 (2000).
[27] K. Hiro, Z. Haibo, and Z. Dan, *Plasma Electronics Engineering* (OHM, 2002).
[28] M. Liu, X. Hu, Z. Jiang, Z. Shu, C. Lan, and P. Yuan, Plasma Sources Sci. Technol. **16**(3), 614 (2007).
[29] K. Takahashi, Y. Shida, and T. Fujiwara, Plasma Sources Sci. Technol. **19**(2), 025004 (2010).
[30] M. A. Lieberman and A. J. Lichtenberg, *Principles of Plasma Discharges and Materials Processing* (Wiley Online Library, 2005).
[31] G. J. M. Hagelaar and L. C. Pitchford, Plasma Sources Sci. Technol. **14**(4), 722–733 (2005).
[32] G. J. M. Hagelaar, K. Makasheva, L. Garrigues, and J. P. Boeuf, J. Phys. D: Appl. Phys. **42**(19), 194019–194030 (2009).
[33] D. P. Lymberopoulos and D. J. Economou, J. Appl. Phys. **73**(8), 3668–3679 (1993).
[34] D. P. Lymberopoulos and D. J. Economou, Appl. Phys. Lett. **63**(18), 2478–2480 (1993).
[35] S. Hübner, J. Wolthuis, J. Palomares, and J. Van der Mullen, J. Phys. D: Appl. Phys. **44**(38), 385202 (2011).
[36] L. Chen, Y. Meng, X. Zuo, Z. Ren, K. Wu, and S. Wang, Plasma Sci. Technol. **17**(5), 372–383 (2015).
[37] L. Guo-wei, M.Sc. thesis, Wuhan Institute of Technology, 2015.
[38] D. Liu, B. Sun, F. Iza, D. Xu, X. Wang, M. Rong, and M. G. Kong, Plasma Sources Sci. Technol. **26**(4), 045009 (2017).
[39] M. Van de Sanden, J. De Regt, and D. Schram, Plasma Sources Sci. Technol. **3**(4), 501 (1994).

23 January 2025 08:35:32

© Author(s) 2020